Noncoalescence of Sessile Drops from Different but Miscible Liquids: Hydrodynamic Analysis of the Twin Drop Contour as a Self-Stabilizing Traveling Wave

Stefan Karpitschka and Hans Riegler

Max-Planck-Institut für Kolloid- und Grenzflächenforschung, Potsdam-Golm, Germany

(Received 30 March 2012; revised manuscript received 16 June 2012; published 10 August 2012)

Capillarity always favors drop fusion. Nevertheless, sessile drops from different but completely miscible liquids often do not fuse instantaneously upon contact. Rather, intermediate noncoalescence is observed. Two separate drop bodies, connected by a thin liquid neck, move over the substrate. Supported by new experimental data, a thin film hydrodynamic analysis of this state is presented. Presumably advective and diffusive volume fluxes in the neck region establish a localized and temporarily stable surface tension gradient. This induces a local surface (Marangoni) flow that stabilizes a traveling wave, i.e., the observed moving twin drop configuration. The theoretical predictions are in excellent agreement with the experimental findings.

DOI: 10.1103/PhysRevLett.109.066103 PACS numbers: 68.03.Kn, 68.03.Cd, 68.08.Bc, 83.10.Bb

Introduction.—Basic physics tells us that two sessile drops will coalesce after contact because of the reduced interfacial energy for a single drop. This instantaneous coalescence has been studied for identical liquids [1,2]. Yet, little is known about the fusion of drops with different but completely miscible liquids, which can be fundamentally different [3–5]: Fusion can be delayed for a long time. After contact, the drops remain separated in a temporary state of noncoalescence, connected only through a thin liquid bridge. This "twin drop configuration" moves over the surface (Fig. 1). Presumably, a Marangoni flow resulting from the surface energy difference of the two liquids causes the noncoalescence [3,4]. An adequate hydrodynamic explanation is still missing. Especially, it is still unclear how a temporarily stationary Marangoni flow forms, stabilizes the noncoalescence, and moves the twin drops.

We present new experimental data and the first analytical hydrodynamic explanation, showing that moving twin drops are a special case of temporarily stationary, self-stabilizing, thin film waves driven by local surface tension gradients. The interaction of drops of different composition is relevant in microfluidics [6,7], and especially so for surface cleaning ("Marangoni drying" [8]).

Experimental results.—Figure 1 shows (see [4] for experimental details) (a) schematically, the experimental setup; (b) the neck in detail: capillarity fills the neck from both sides, whereas Marangoni sucks out liquid asymmetrically, thus moving the drops with v_N and preventing coalescence (see Supplemental Material [9]); (c) noncoalescence [10]; and (d) drops from identical liquids fusing instantaneously upon contact. With sufficiently different surface tensions (c), the drops do not fuse. The main drop bodies $[h''(x) < 0]$ stay separated in a temporary state of noncoalescence, connected by a thin liquid neck $[h''(x) \gg 0]$. The noncoalescing twin drops move over the substrate with constant velocity, almost independent from $\Delta\gamma$ (Fig. 2). Through the neck, small amounts of liquid flow from drop 2 (lower surface tension, γ_2) to drop 1 ($\gamma_1 > \gamma_2$), slowly reducing the surface energy difference $\Delta\gamma = \gamma_1 - \gamma_2$. Eventually, the drops merge (delayed up to minutes [4]).

Flow patterns were investigated by imaging dispersed fluorescent polystyrene microspheres (Duke Scientific, $d = 1\ \mu$m, mass fraction $\approx 2.4 \times 10^{-7}$). Figure 3 shows their traces in the neck region (see Supplemental Material [9]). In the substrate frame, all microspheres move from left to right. At or near the liquid-air interface of drop 2, the spheres move with $\approx \frac{3}{2} v_N$ (positions 1 and 2). Close to the neck, they touch the substrate ($d \approx$ neck height h) and slow down (position 3). On the other side of the neck, in drop 1, those spheres that were at rest close to the substrate (position 4) get uplifted by the liquid flow through the neck. Spheres at the liquid-air interface of drop 1 can reach up to $\approx 2v_N$ (position 5). While moving away from the neck region, their speed slows down to $\approx \frac{3}{2} v_N$ (position 6).

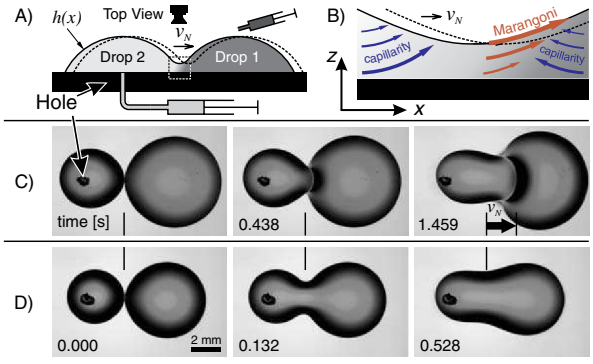

FIG. 1 (color online). (a) Schematics of the experimental setup or procedure; (b) flow scheme of the neck region; (c) noncoalescent twin drop movement (different, miscible liquids); (d) instantaneous coalescence (identical liquids).

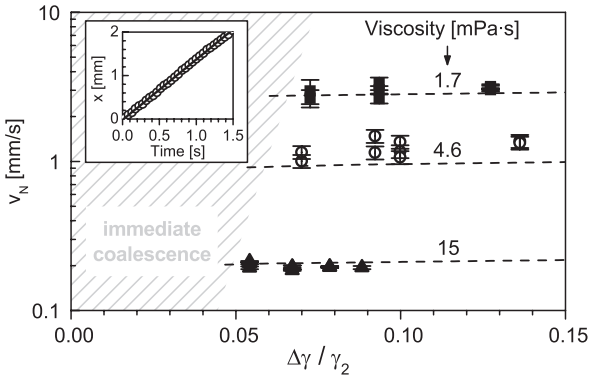

FIG. 2. Neck displacement velocity v_N versus surface energy difference $\Delta\gamma/\gamma_2$ (the inset demonstrates the constancy of v_N). Dashed lines: Analytically calculated v_N (see also Fig. 5), in quantitative agreement with experiments.

As discussed below, the speed component in addition to $\frac{3}{2}v_N$ is caused by the local Marangoni flow.

Hydrodynamic model.—The steady-state twin drop movement is analyzed by assuming a viscous, laminar Newtonian flow (no slip, no gravity, lubrication approximation). The two drops are approximated by cross sections through two infinitely long cylinders, connected by a thin neck, moving with constant speed and stationary shape. They consist of miscible liquids with different surface tensions. The liquid with the lower surface tension continuously flows through the neck into drop 1. Diffusive-advective mixing establishes a local stationary composition profile because the volume exchange per time is small compared to the overall drop volumes. The composition profile causes a local surface tension gradient on drop 1 close to the neck (for a detailed qualitative description of how the Marangoni flow resulting from this gradient stabilizes stationary noncoalescence, see Supplemental Material [9]).

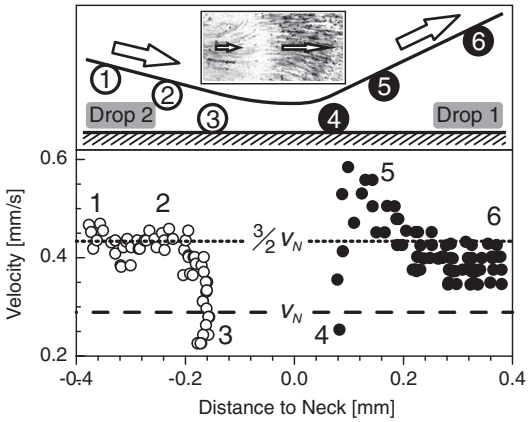

FIG. 3. Flow velocities (substrate frame) of individual microspheres as a function of their distance to the neck (moving twin drops, open circles: upstream, drop 2; closed circles: downstream, drop 1). Dashed line: Measured neck velocity v_N. Speeds exceeding $\frac{3}{2}v_N$ indicate a (local) surface tension gradient.

The (stationary) surface topology $h(x)$ of a liquid film with surface tension $\gamma(x)$, moving on a solid support with capillary number $\mathrm{Ca} = \eta v_N/\gamma$, is described by the balance between changes of the surface curvature, viscous dissipation, and surface energy gradients [11]:

$$h''' = 3\mathrm{Ca}/h^2 - 3\gamma'/(2h\gamma). \tag{1}$$

Without the Marangoni term ($\gamma' = 0$), Eq. (1) cannot describe a stationary twin-drop profile, because $h''' > 0$ allows only one inflection point (one drop connected to a neck). However, with $\gamma' \neq 0$, a second inflection point, i.e., a second drop, can exist, because h''' may change sign.

The velocity field $u(z)$ within the film is [11]

$$u = z/\eta[\gamma' - (z/2 - h)\gamma h'''] . \tag{2}$$

Equations (1) and (2) yield the surface flow velocity ($z = h$)

$$u_s = u|_{z=h} = 3v_N/2 + h\gamma'/(4\eta). \tag{3}$$

The Marangoni component increases u_s, and by sucking liquid out of the neck region, it favors noncoalescence.

This explains the experimental results (Fig. 3). For drop 2, the maximum (surface-)velocity is $\approx \frac{3}{2}v_N$ (i.e., no surface tension gradient). However, at the surface of drop 1, close to the neck, $u_s > \frac{3}{2}v_N$; i.e., $\gamma' \neq 0$. Liquid 2 flows through the neck, causing a localized gradient next to the neck (≈ 0.2 mm, drop sizes >mm).

Localized surface tension gradient.—Marangoni forces cause the flow through the neck: they "pull" liquid 2 as a thin film onto drop 1 where it mixes with liquid 1. This is approximated by a layer of liquid 2 with thickness h_N spreading onto drop 1 with a velocity $\frac{3}{2}v_N$ [12], where it is diluted by diffusion. Compared to the influx of liquid 2, drop 1 is a large reservoir of liquid 1. Therefore, the dilution is approximately stationary.

With negligible diffusion in flow direction, this is described by the stationary advection-diffusion equation. In the (moving) contour frame, the advection velocity is $v_N/2$:

$$D\frac{\partial^2 c}{\partial z^2} = \frac{v_N}{2}\frac{\partial c}{\partial x}, \tag{4}$$

with D = diffusivity and local compositions $c \in [0, 1]$ from pure liquid 1 to pure liquid 2, respectively; $c|_{x=0} = 1$ for $0 < z < 2h_N$ and 0 elsewhere ($2h$ assures $\partial c/\partial z|_{z=h_N} = 0$, i.e., nonvolatile liquids); $\gamma(x)$ shall depend locally on $c(x, z)$ with $\gamma(x) = \gamma_2 + \Delta\gamma c(x, h)$. Then, the solution to Eq. (4) yields

$$\gamma' = \frac{\Delta\gamma}{2h_N}\sqrt{\frac{\mathrm{Bo}}{2\pi}}(x/h_N)^{-3/2}\exp\left[-\frac{\mathrm{Bo}}{8}x/h_N\right]. \tag{5}$$

With Bodenstein number $\mathrm{Bo} = v_N h_N/D$ (a Péclet number with advection and diffusion orthogonal); $\gamma'_{\max}$ is

at $x_{\max} = \mathrm{Bo}h_N/12$, with $\Delta x_{\mathrm{FWHM}} \approx 0.225\mathrm{Bo}h_N$ (Fig. 4). With typical experimental parameters ($v_N \approx 1$ mm/s, $h_N \approx 10$ μm, $D \approx 10^{-10}$ m^2/s), γ' is $\neq 0$ only close to the neck ($x_{\max} \approx 0.08$ mm, $\Delta x_{\mathrm{FWHM}} \approx 0.2$ mm). This and the typical experimental values of $\Delta\gamma \lesssim 0.1\gamma_2$ justifies assuming $\gamma(x) \approx \gamma_2$ whenever $\gamma(x)$ is used explicitly.

Inserting Eq. (5) and (1) is solved numerically. The result (Fig. 4, solid red lines) matches the experimental findings (explicitly shown in [4,5]). It reveals moving twin drops driven by a surface tension gradient. The contours for drop 2 as well as for the main body of drop 1 are described by Eq. (1) with $\gamma' = 0$. This, together with the surface tension gradient localized to the neck section, is the key to the following analysis, which relates v_N to measurable quantities.

Analytical approach.—With $\gamma' \neq 0$ limited to the neck region of drop 1, the drop bodies themselves can be described by Eq. (1) with $\gamma' = 0$. Analytic solutions describing a (single) drop contour can be parametrized around a local extremum ($s = s_2$, $x = 0$, and $h = h_N$; see Fig. 4, dashed lines) [13–15]:

$$x_{\gamma'=0}(s) = \frac{h_N[\mathrm{Ai}(s)\mathrm{Bi}(s_2) - \mathrm{Ai}(s_2)\mathrm{Bi}(s)]}{(3\mathrm{Ca}/2)^{1/3} p_{s_2}(s)}, \tag{6}$$

$$h_{\gamma'=0}(s) = h_N/[\pi p_{s_2}(s)]^2, \tag{7}$$

with $p_{s_2}(s) = \mathrm{Ai}(s)\mathrm{Bi}'(s_2) - \mathrm{Ai}'(s_2)\mathrm{Bi}(s)$. For $s_2 \in [-1.01879, 0]$, Eqs. (6) and (7) show a local minimum at $s = s_2$. The position of the receding contact line is $x_r = h_N(\frac{3}{2}\,\mathrm{Ca})^{-1/3}\mathrm{Ai}(s_2)/\mathrm{Ai}'(s_2)$. On the right, at $x = 0$, the drop contour is connected through a neck (height h_N) to an infinite liquid volume: the contour diverges at $x > 0$.

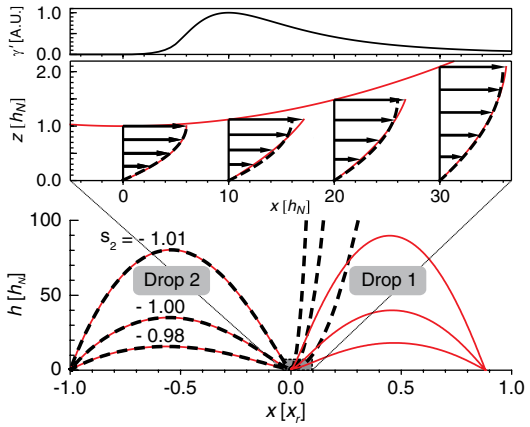

FIG. 4 (color online). Moving drop contours with different shape parameters s_2. Dashed black lines: Analytical solutions for homogeneous surface tension (single drop). Solid red lines: Noncoalescing twin drop contour (numerical solution) for a localized surface tension gradient γ' (top panel), and the corresponding velocity field (middle).

At the branch limit $s = s^{(\infty)} \approx -1.732 + 0.595s_2$ (see, e.g., [14] for details), both $x_{\gamma'=0} \to \infty$ and $h_{\gamma'=0} \to \infty$.

We assume that Eqs. (6) and (7) for $x < 0$ individually describe the main bodies of drop 2 and drop 1, respectively. To compose the twin drop contour from these, we suppose that the contour of drop 2 is modified at $x > 0$ (i.e., to the right of the neck in Fig. 4) by the local gradient γ' [see Eq. (5)]. This modification does not affect the gradient-free upstream contour section [Eqs. (6) and (7) for $x < 0$]. Instead, the local gradient γ' affects the asymptotic curvature for $x \to \infty$, far away from the neck. This gradient-modified curvature is then matched to the apex curvature of another (gradient-free) drop contour for drop 1. At the apex of drop 1, the curvature is always negative, whereas for Eqs. (6) and (7) for $x > 0$ (without gradient), $h'' > 0$. Therefore, to match both curvatures, a local gradient must be sufficiently "strong" to establish a negative curvature for $x > 0$. Then, such matching links the parameters of the individual solutions to a twin drop configuration.

The curvature at the neck ($x = 0$) is derived from Eqs. (6) and (7):

$$h''_{\gamma'=0}(x = 0) = -2(3\mathrm{Ca}/2)^{2/3} s_2/h_N. \tag{8}$$

For $x_{\gamma'=0} \to \infty$ (the diverging contour section), the curvature is finite and positive:

$$h''_{\gamma'=0}(x \to \infty) = 2\pi^2(3\mathrm{Ca}/2)^{2/3} p'_{s_2}(s^{(\infty)})^2/h_N. \tag{9}$$

With $\gamma' \neq 0$ restricted to the neck region at $x > 0$, the curvature change can be approximated:

$$h''_\infty \approx h''_{\gamma'=0}(x \to \infty) - \frac{3}{2\gamma_2}\int_0^\infty \frac{\gamma'}{h_{\gamma'=0}}\,dx. \tag{10}$$

Here, the true $h(x)$ is approximated by $h_{\gamma'=0}$, the contour without gradient. Of course, if we assume a significant impact of the local $\gamma'(x)$, at some distance from the neck, h will be different from $h_{\gamma'=0}$. However, $\gamma'(x)$ is localized and $h(x)$ grows quickly. Thus, with increasing distance from the neck, $\gamma'/h_{\gamma'=0}$ (the integrand) rapidly becomes negligible: the integral error remains small, and the upper integration limit is irrelevant and can be set to infinity (see Supplemental Material [9]). Eq. (10) is integrated analytically by expanding $h_{\gamma'=0}(x)$ around $x = 0$ to second order [see Eq. (8)]:

$$\frac{3}{2\gamma_2}\int_0^\infty \frac{\gamma'}{h_{\gamma'=0}}\,dx \approx \frac{3\Delta\tilde{\gamma}}{2h_N} q(k)^{-1}. \tag{11}$$

Here, $k = \mathrm{Bo}(\frac{3}{2}\,\mathrm{Ca})^{1/3}\sqrt{-s_2}$ and $\Delta\tilde{\gamma} \approx \Delta\gamma/\gamma_2$. $q(k)$ is lengthy (see Supplemental Material [9]), but (for typical parameters) can well be approximated in powers of k: $q(k) \approx 1 + \sqrt{\pi k}/4 + k(\pi + k/3)/16$. Eqs. (10) and (11) yield:

$$h''_\infty \approx \frac{2}{h_N}\left[\pi^2(3\mathrm{Ca}/2)^{2/3} p'_{s_2}(s^{(\infty)})^2 - \frac{3\Delta\tilde{\gamma}}{4} q(k)^{-1}\right]. \tag{12}$$

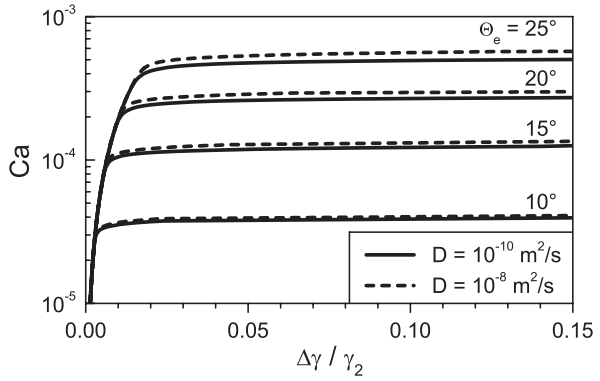

FIG. 5. Capillary number for noncoalescing drops (contact angles $\Theta_e = \Theta_{e,2} = \Theta_{e,1}$) versus surface tension difference $\Delta\gamma/\gamma_2$.

The second term indicates that the asymptotic curvature may indeed become negative for sufficiently large $\Delta\tilde{\gamma}$.

Equation (12) estimates the asymptotic curvature for $x \to \infty$ as a function of a local gradient. For a twin drop configuration, it shall match the apex curvature of a gradient-free drop (drop 1), described by Eqs. (6) and (7) [replacing h_N by h_1 and s_2 by s_1, with $s_1 > 0$ to parametrize at the apex instead of the neck. The apex curvature is given by the corresponding Eq. (8)].

Moving twin drops with a stationary contour means identical capillary numbers Ca, yielding

$$\Delta\tilde{\gamma} = 4/3(3\mathrm{Ca}/2)^{2/3} q(k)[h_N s_1/h_1 + \pi^2 p'_{s_2}(s^{(\infty)})^2]. \quad (13)$$

Equation (13) contains the parameters s_2, s_1, h_N, and h_1 (and implicitly Bo), which represent experimental parameters, such as the static equilibrium contact angles $\Theta_{e,1}$ and $\Theta_{e,2}$, the drop volumes (= areas A_1 and A_2 under the drop contours), and D. The contour area A_2 ($x < 0$) is connected to h_N by

$$A_2 = (3\mathrm{Ca}/2)^{-1/3} \frac{h_N^2}{\pi^4} \int_{s_2}^{\infty} p_{s_2}(s)^{-4} ds. \quad (14)$$

Matching the receding contact line to a microscopic solution [15,16] gives s_2 as a function of Ca, with $\Theta_{e,2}$ and a slip length λ_c (besides A_2) as parameters:

$$\mathrm{Ai}'(s_2) = \frac{\Theta_{e,2} h_N}{6\pi\lambda_c} (3\mathrm{Ca}/2)^{-1/3} \exp\left[-\frac{\Theta_{e,2}^3}{9\mathrm{Ca}}\right]. \quad (15)$$

Matching the advancing contact line of drop 1 to a microscopic solution [inflection point of Eqs. (6) and (7) approximated by $s_i \approx s_1 - 1$] yields [15]

$$\Theta_{e,1} \approx -(12\mathrm{Ca})^{1/3} \sqrt{s_1 - 1} \tanh\tfrac{2}{3}[(s_1 - 1)^{3/2} - s_1^{3/2}]. \quad (16)$$

A_1 for drop 1 determines the apex height h_1 [Eq. (14) with suitable integration limits].

Now the system is closed. $\Delta\tilde{\gamma}$ propelling the drops with Ca results from inserting solutions to Eqs. (14)–(16) into Eq. (13). Figure 5 presents the ensuing Ca as a function of $\Delta\tilde{\gamma}$ for various Θ_e (assuming $\Theta_e = \Theta_{e,2} = \Theta_{e,1}$). Experimentally this means, the given combinations of Θ_e and $\Delta\tilde{\gamma}$ result in a certain Ca; i.e., the twin drops move at a certain speed. Theoretical (Fig. 5) and experimental (Fig. 2) findings agree quantitatively (within $\approx 10\%$). Both show that v_N is approximately independent from $\Delta\tilde{\gamma}$ (which is counterintuitive; $\Delta\tilde{\gamma}$ is obviously the source for the motion). The analysis predicts that the contact angles determine the order of magnitude for Ca. Assuming experimentally realistic conditions, the other parameters change Ca by less than $\pm 25\%$. As depicted, changing D by a factor of 100 (e.g., due to shear-induced dispersion; see Supplemental Material [9]) barely affects Ca. Different, absolute, or relative drop sizes also have little influence, because the (large) neck curvature dominates the capillarity (not the much smaller drop curvatures).

The analysis leading to Fig. 5 assumes stationary conditions. This requires large drop volumes so that the flow between drop 2 and drop 1 changes the composition of drop 1 and, thus, $\Delta\tilde{\gamma}$, only slowly. Also, $\Delta\tilde{\gamma}$ has to be sufficiently large so that the minor changes in $\Delta\tilde{\gamma}$ barely change Ca, and v_N is approximately constant (horizontal sections of Ca vs $\Delta\tilde{\gamma}$ in Fig. 5). The range where Ca decreases rapidly with decreasing $\Delta\tilde{\gamma}$ is quantitatively not covered by our analytical approach. Experimentally, immediate coalescence is observed here. Nevertheless, via the flow through the neck, we can estimate the lifetime of the noncoalescence (see Supplemental Material [9]) (which agrees well with the experiments).

Conclusion.—We present new experimental data of noncoalescing sessile twin drops from different miscible liquids. In a thin film approximation, they are described as two moving drops that are connected by a liquid neck. Through this neck, liquid flows from the upstream to the downstream drop. An advection-diffusion balance establishes a localized, (temporarily) stable surface tension gradient close to the neck, which causes a Marangoni flow that sucks liquid out of the neck. This counteracts the capillary-driven flow into the neck and thus stabilizes noncoalescence. The whole system forms a self-stabilizing, traveling wave (twin-drop contour). The theoretical predictions are in quantitative agreement with the experimental findings.

We thank H. Möhwald for scientific advice and general support and L. Pismen for helpful discussions, in particular suggesting an approach via Eq. (6). S. K. was supported by the DFG (RI529/16-1).

[1] D. Aarts, H. Lekkerkerker, H. Guo, G. Wegdam, and D. Bonn, Phys. Rev. Lett. **95**, 164503 (2005).
[2] W. Ristenpart, P. McCalla, R. Roy, and H. Stone, Phys. Rev. Lett. **97**, 064501 (2006).
[3] H. Riegler and P. Lazar, Langmuir **24**, 6395 (2008).
[4] S. Karpitschka and H. Riegler, Langmuir **26**, 11 823 (2010).
[5] R. Borcia, S. Menzel, M. Bestehorn, S. Karpitschka, and H. Riegler, Eur. Phys. J. E **34**, 24 (2011).

[6] Y.-H. Lai, M.-H. Hsu, and J.-T. Yang, Lab Chip **10**, 3149 (2010).
[7] Z. G. Li, K. Ando, J. Q. Yu, A. Liu, J. Zhang, and C. Ohl, Lab Chip **11**, 1879 (2011).
[8] A. Leenaars, J. Huethorst, and J. van Oekel, Langmuir **6**, 1701 (1990).
[9] See Supplemental Material at http://link.aps.org/supplemental/10.1103/PhysRevLett.109.066103 for videos, a mechanistic description, an estimation of Taylor-Aris dispersion, and additional information on mathematical details.
[10] Liquids: ternary mixtures of 1,2-, 1,3-propanediol, and water (50% of total mass, viscosity $\eta_1 \approx \eta_2 \approx 4.6$ cP). $\Delta\gamma$ was tuned by varying relative amounts of diols. Sequence B: identical liquids (1, 2-propanediol + water, $\gamma_1 = \gamma_2 \approx 44.9$ mN/m). Sequence C: drop 2 as before; drop 1: 18.8% 1,2- and 31.2% 1,3-propanediol; $\Delta\gamma \approx 6.1$ mN/m.
[11] A. Oron, S. Davis, and S. Bankoff, Rev. Mod. Phys. **69**, 931 (1997).
[12] In experiments, the γ' contribution to u_s was always significantly smaller than $\frac{3}{2}v_N$.
[13] W. Ford, SIAM Rev. **34**, 121 (1992).
[14] B. Duffy and S. Wilson, Appl. Math. Lett. **10**, 63 (1997).
[15] L. Pismen and U. Thiele, Phys. Fluids **18**, 042104 (2006).
[16] J. Eggers, Phys. Rev. Lett. **93**, 094502 (2004).